Available online at www.sciencedirect.com
SCIENCE DIRECT®
Comput. Methods Appl. Mech. Engrg. 193 (2004) 3523–3540
Computer methods in applied mechanics and engineering
www.elsevier.com/locate/cma

A finite element method for the simulation of strong and weak discontinuities in solid mechanics

Anita Hansbo [a], Peter Hansbo [b,*]

[a] Department of Informatics and Mathematics, University of Trollhättan Uddevalla, Box 957, S-461 39 Trollhättan, Sweden
[b] Department of Applied Mechanics, Chalmers University of Technology, S-412 96 Göteborg, Sweden

Received 18 April 2003; received in revised form 27 November 2003; accepted 9 December 2003

Abstract

In this paper we introduce and analyze a finite element method for elasticity problems with interfaces. The method allows for discontinuities, internal to the elements, in the approximation across the interface. We propose a general approach that can handle both perfectly and imperfectly bonded interfaces without modifications of the code. For the case of linear elasticity, we show that optimal order of convergence holds without restrictions on the location of the interface relative to the mesh. We present numerical examples for the linear case as well as for contact and crack propagation model problems.

Keywords: Finite element method; Discontinuities; Solid mechanics

1. Introduction

As a model inclusion problem, we consider a linear elasticity problem in two or three dimensions with stiffness and/or Poisson's ratio discontinuous across a smooth internal interface. The interface is assumed to be perfectly bonded or, alternatively, imperfectly bonded with elastic spring-type interface conditions. We also consider a combination of the two to allow for self-contact, which yields a non-linear Signorini-type problem.

When solving such problems numerically using the standard finite element method, one usually takes the discontinuity of the data into account by enforcing mesh lines along the interface. If this is not done, suboptimal convergence behaviour will occur, cf. [1]. In contrast, the method introduced here is an extension of the unfitted finite element method presented in [4], allowing for discontinuities, *internal* to the elements, in the approximation across the interface separating the inclusion from the rest of the domain.

Another interesting feature of our method is its capability to handle both perfectly and imperfectly bonded interfaces with small or large compliancy. This is accomplished by using a non-standard bilinear

* Corresponding author. Fax: +46-31-772-3827.
E-mail address: hansbo@solid.chalmers.se (P. Hansbo).

0045-7825/$ - see front matter © 2004 Elsevier B.V. All rights reserved.
doi:10.1016/j.cma.2003.12.041

form to define the method, together with a suitably chosen penalty parameter which depends on the interface conditions as well as on the mesh. We will show that the method is of optimal order of convergence, and, moreover, that the convergence is uniform with respect to the compliancy at the interface.

The possibility of incorporating discontinuities, either weak (discontinuous strains) or strong (discontinuous displacement fields) has been considered by several authors recently. Among the approaches most similar to ours we mention the partition of unity methods of Belytschko and co-workers [2] and of Wells and Sluys [9]. For an overview of recent work in this field, with many additional references, see Karihaloo and Xiao [5]. In [9] only strong discontinuities are considered, since the jump is an explicit variable. The suboptimal convergence behaviour in the presence of weak discontinuities is thus still present with this method. By use of signed distance functions, the approach in [2] can handle weak discontinuities, with the strain jump as an explicit variable. In contrast, our approach is more like "traditional" finite element methods in that we only work with polynomial approximations, and neither the jump nor the strain jump is an explicit variable. We instead allow for discontinuities in the solution, and enforce the continuity in tractions (and, if applicable, displacements) only in a weak sense. The rate of convergence for the methods [2,9] is not known; to the best of our knowledge the present work is the first to show optimally convergent approximations of weak and strong discontinuities for elasticity problems.

A compressible linear elasticity model problem with a perfectly or imperfectly bonded interface is presented in Section 2. The proposed finite element method is defined in Section 3, and Section 4 contains its convergence analysis. In Section 5, we provide numerical examples that confirm the optimal convergence rate in the linear case and indicate the feasibility of our approach applied to contact and fracture model problems, and finally, in Section 6, some concluding remarks are given.

2. A linear elasticity problem with debonding at the interface

In many cases, typically when the interface consists of a thin layer of adhesive, there is a need to model imperfect bonding at the interface. We begin by presenting an unfitted finite element method for this case. In order to have a linear model problem, we do not allow for self-contact; we shall return to this question in Section 5.2.

2.1. Problem formulation and notation

Let Ω be a bounded domain in $\mathbb{R}^n$, $n = 2$ or $n = 3$, with convex polygonal boundary $\partial\Omega$ and an internal smooth boundary Γ dividing Ω into two open sets Ω_1 and Ω_2. Throughout this paper we shall use subscripts to denote the restriction of a function to Ω_i. Vectors and tensors are typed in bold face and superscripts are used for their components. Thus, $\boldsymbol{u} = [u^i]_{i=1}^n$ may denote a vector valued function in Ω with components u^i, while $\boldsymbol{u}_i = \boldsymbol{u}|_{\Omega_i}$ denotes its restriction to Ω_i. For any sufficiently regular function $\boldsymbol{u}$ in $\Omega_1 \cup \Omega_2$ we define the jump of $\boldsymbol{u}$ on Γ by $[\boldsymbol{u}] := \boldsymbol{u}_1|_\Gamma - \boldsymbol{u}_2|_\Gamma$. Conversely, for $\boldsymbol{u}_i$ defined in Ω_i we identify the pair $\{\boldsymbol{u}_1, \boldsymbol{u}_2\}$ with the function $\boldsymbol{u}$ which equals $\boldsymbol{u}_i$ on Ω_i.

For a bounded open connected domain D we shall use standard Sobolev spaces $H^r(D)$ with norm $\|\cdot\|_{r,D}$ and spaces $H_0^r(D)$ with zero trace on ∂D. The inner products in $H^0(D) = L_2(D)$ is denoted $(\cdot,\cdot)_D$. For a bounded open set $G = \cup_{i=1}^2 D_i$, where D_i are open mutually disjoint components of G, we let $H^k(D_1 \cup D_2)$ denote the Sobolev space of functions in G such that $\boldsymbol{u}|_{D_i} \in [H^k(D_i)]^n$ with norm

$$\|\cdot\|_{k,D_1\cup D_2} = \left(\sum_{i=1}^{2} \|\cdot\|_{k,D_i}^2 \right)^{1/2}.$$

We shall use c and C below to denote generic constants, not necessarily the same at each occurrence.

We consider the following elasticity problem with a discontinuity in the Lamé parameters across Γ: Find the displacement $\boldsymbol{u}$ and the symmetric stress tensor $\boldsymbol{\sigma} = [\sigma^{ij}]_{i,j=1}^{n}$ such that

$$\begin{aligned} \boldsymbol{\sigma} &= \lambda \nabla \cdot \boldsymbol{u} \boldsymbol{I} + 2\mu \boldsymbol{\varepsilon}(\boldsymbol{u}) && \text{in } \Omega_1 \cup \Omega_2, \\ -\nabla \cdot \boldsymbol{\sigma} &= \boldsymbol{f} && \text{in } \Omega_1 \cup \Omega_2, \\ \boldsymbol{u} &= 0 && \text{on } \partial\Omega, \\ [\boldsymbol{\sigma} \cdot \boldsymbol{n}] &= 0 && \text{on } \Gamma, \\ [\boldsymbol{u}] &= -\boldsymbol{K}\boldsymbol{\sigma} \cdot \boldsymbol{n} && \text{on } \Gamma, \end{aligned} \tag{1}$$

where the load $\boldsymbol{f} \in [L_2(\Omega)]^n$. Here λ and μ are the Lamé parameters, which we assume satisfy $0 < c < \mu < C$ and $0 < \lambda < C$; thus we exclude the incompressible case. In terms of the modulus of elasticity, E, and Poisson's ratio, v, we have

$$\lambda = \frac{Ev}{(1-2v)(1+v)}, \quad \mu = \frac{E}{2(1+v)}.$$

Furthermore, $\boldsymbol{\varepsilon}(\boldsymbol{u}) = [\varepsilon^{ij}(\boldsymbol{u})]_{i,j=1}^{n}$ is the strain tensor with components

$$\varepsilon^{ij}(\boldsymbol{u}) = \frac{1}{2}\left(\frac{\partial u^i}{\partial x^j} + \frac{\partial u^j}{\partial x^i}\right),$$

$\nabla \cdot \boldsymbol{\sigma} = [\sum_{j=1}^{2} \partial\sigma^{ij}/\partial x^j]_{i=1}^{n}$, $\boldsymbol{I} = [\delta^{ij}]_{i,j=1}^{n}$ with $\delta^{ij} = 1$ if $i = j$ and $\delta^{ij} = 0$ if $i \neq j$, and $\boldsymbol{n}$ is the outward normal to Ω_1. Finally, $\boldsymbol{K}$ is a positive semi-definite tensor representing the compliancy of the interface. We consider here only isotropic elasticity on the interface, in which case we can write

$$\boldsymbol{K} = \alpha \boldsymbol{I} + (\beta - \alpha)\boldsymbol{n} \otimes \boldsymbol{n}, \quad \text{or} \quad K^{ij} = \alpha\delta^{ij} + (\beta - \alpha)n^i n^j,$$

with $\alpha \geqslant 0$ and $\beta \geqslant 0$ denoting the compliancy in the direction tangential and normal to the interface, respectively [10]. For simplicity, we assume that λ and μ are constant in Ω_i, and that $\boldsymbol{K}$ is constant on Γ.

Let the interface stiffness S be defined by

$$\boldsymbol{S} = \begin{cases} \boldsymbol{K}^{-1} & \text{for } \alpha > 0, \beta > 0, \\ \alpha^{-2}\boldsymbol{K} = \alpha^{-1}(\boldsymbol{I} - \boldsymbol{n} \otimes \boldsymbol{n}) & \text{for } \alpha > 0, \beta = 0, \\ \beta^{-2}\boldsymbol{K} = \beta^{-1}\boldsymbol{n} \otimes \boldsymbol{n} & \text{for } \alpha = 0, \beta > 0, \\ 0 & \text{for } \alpha = 0, \beta = 0, \end{cases}$$

and define the space V of test functions by

$$V = \{\boldsymbol{v} \in V_1 \times V_2 : [\boldsymbol{v}] = \boldsymbol{S}\boldsymbol{K}[\boldsymbol{v}]\} \quad \text{where } V_i = \{\boldsymbol{v}_i \in [H^1(\Omega_i)]^n : \boldsymbol{v}_i|_{\partial\Omega} = 0\}.$$

Note that when $\boldsymbol{S} = \boldsymbol{K}^{-1}$ then $V = V_1 \times V_2$. A weak form of (1) may be formulated as follows: find $\boldsymbol{u} = (\boldsymbol{u}_1, \boldsymbol{u}_2) \in V$ such that

$$a_{\boldsymbol{S}}(\boldsymbol{u}, \boldsymbol{v}) = L(\boldsymbol{v}) \quad \forall \boldsymbol{v} \in V. \tag{2}$$

Here,

$$a_{\boldsymbol{S}}(\boldsymbol{u}, \boldsymbol{v}) := (\boldsymbol{\sigma}(\boldsymbol{u}), \boldsymbol{\varepsilon}(\boldsymbol{v}))_{\Omega_1 \cup \Omega_2} + (\boldsymbol{S}[\boldsymbol{u}], [\boldsymbol{v}])_{\Gamma},$$

where

$$(\boldsymbol{\sigma}, \boldsymbol{\varepsilon})_{\Omega_i} = \int_{\Omega_i} \boldsymbol{\sigma} : \boldsymbol{\varepsilon} \, \mathrm{d}x = \int_{\Omega_i} \sum_{kl} \sigma^{kl}\varepsilon^{kl} \, \mathrm{d}x,$$

and

$$L(\boldsymbol{v}) := (\boldsymbol{f}, \boldsymbol{v})_{\Omega}.$$

The solution to this problem is in H^2 on each subdomain Ω_i, cf. Leguillon and Sanchez-Palencia [6].

3. A finite element method with interelement discontinuities for perfectly and imperfectly bonded interfaces

For the problem under consideration, we shall define an approximation method which is capable of handling (1) for all interface conditions considered. As we shall see, this method is optimal order convergent for strongly as well as for weakly discontinuous solutions of this problem.

In a standard conforming finite element method, the possibility of jumps in the strain across the interface can be taken into account by letting Γ coincide with mesh lines. Here, we instead use discontinuous approximations over the interface in order to accommodate possible strong discontinuities in the solution. Moreover, we shall allow the approximation to be discontinuous *inside* elements which intersect the interface. We will follow [4] and solve (1) approximately using piecewise linear finite elements on a family of conforming triangulations T_h of Ω which are independent of the location of the interface Γ.

3.1. Elements with internal discontinuities

We will first explain how elements with internal discontinuities are constructed from standard (in the simplest case linear) finite elements on a triangular grid in the plane. Consider an element K which is intersected by the interface and thus consists of one part $K_1 := \Omega_1 \cap K$ in Ω_1, and another part $K_2 := \Omega_2 \cap K$ in Ω_2. FE functions ϕ with internal discontinuities in K will be linear on each part but discontinuous over Γ. Thus

$$\phi = \begin{cases} \phi_1 & \text{in } K_1, \\ \phi_2 & \text{in } K_2. \end{cases}$$

Since ϕ is discontinuous over the interface, no relation between (the degrees of freedoms for) ϕ_1 and ϕ_2 is enforced in the definition of the approximating functions. To determine the linear function ϕ_1 on K_1, one needs three degrees of freedom. Notice that we may very well choose to represent ϕ_1 by the nodal values at the corners of K (strictly speaking: represent ϕ_1 by the nodal values of its unique linear extension to K), even though we think of ϕ_1 as not being defined on K_2. Likewise, ϕ_2 lives only on K_2 but we may still represent it by its values in the same three element corner nodes. Thus the piecewise linear element with an internal discontinuity has six degrees of freedom.

A FE basis with inter element discontinuities over the interface is obtained from the standard basis by, for each node on the elements that are intersected by Γ, replacing the standard basis function ψ by two new basis function $\check{\psi}$ and $\hat{\psi}$ as follows. Consider a standard linear basis function ψ that takes on the value one in one of the nodes of K and zero in all other nodes in Ω. If K is intersected by the interface, this standard basis function is replaced by the following new basis functions with discontinuities over the interface:

$$\check{\psi} = \begin{cases} \psi & \text{in } \Omega_1, \\ 0 & \text{in } \Omega_2, \end{cases} \quad \text{and} \quad \hat{\psi} = \begin{cases} 0 & \text{in } \Omega_1, \\ \psi & \text{in } \Omega_2. \end{cases}$$

Clearly, $\check{\psi}$ and $\hat{\psi}$ are continuous functions (over all element edges) in Ω_i.

Turning our attention back to one single element again, we may in this way generate six discontinuous basis functions from the three standard basis functions on the linear element. We get as desired one discontinuous basis function for each degree of freedom on the element with an internal discontinuity.

By similar reasoning, we see that from *any* standard finite element in 2D or 3D, a corresponding element with internal discontinuity across an interface may be constructed. Furthermore, one may do this using the nodes on the standard element to represent the degrees of freedom. The number of degrees of freedom for the element with an internal discontinuity is twice that of the original element, and a FEM basis may be constructed by considering two copies of the original basis functions, restricted to Ω_1 and Ω_2, respectively. When both copies are represented using the same degrees of freedom as the original standard finite element, the geometry of the interface and the element parts does *not* come into play until when integrating the terms in the bilinear form.

Formalizing this tutorial explanation, we shall seek a discrete solution $\boldsymbol{U} = (\boldsymbol{U}_1, \boldsymbol{U}_2)$ in the space $V^h = V_1^h \times V_2^h$, where

$$V_i^h = \{\boldsymbol{\phi}_i \in [H^1(\Omega_i)]^n : \ \boldsymbol{\phi}_i|_{K_i} \text{ is linear}, \ \boldsymbol{\phi}_i|_{\partial\Omega} = 0\}.$$

The functions in V^h may be discontinuous across Γ, and the interface conditions will be imposed weakly. Note, however, that the definition of V^h implies that the finite element functions are continuous over all element sides on either side of Γ.

3.2. Formulation of the method

Now, for $\alpha > 0, \beta > 0$, the continuous problem (2) could simply be approximated by a straightforward use of the discrete space V^h: Find $\boldsymbol{U} \in V^h$ such that

$$a_{\boldsymbol{S}}(\boldsymbol{U}, \boldsymbol{\phi}) := (\boldsymbol{\sigma}(\boldsymbol{U}), \boldsymbol{\varepsilon}(\boldsymbol{\phi}))_{\Omega_1 \cup \Omega_2} + (\boldsymbol{S}[\boldsymbol{U}], [\boldsymbol{\phi}])_\Gamma = L(\boldsymbol{\phi}) \quad \forall \boldsymbol{\phi} \in V^h. \tag{3}$$

However, in the case of small compliancy parameters α and β this would lead to a badly conditioned problem, and, furthermore, the question of locking would have to be considered. This formulation would also fail in the limit case $\alpha = 0$ or $\beta = 0$ since the functions in V^h do not fulfill any interface conditions over Γ. On the other hand, for the case $\alpha = 0$ and $\beta = 0$, the boundary conditions may still be imposed weakly over the interface by using a penalty method, e.g., a consistent Nitsche [7] type method like in [4].

To be able to treat all cases using the same method, we shall here investigate a more general consistent penalty approach. To this end, we shall need to define a numerical stress at the interface. Before giving the details, we introduce our notation for any convex combination of the stresses at each side of the interface. Given $\kappa = (\kappa_1, \kappa_2)$ with $0 \leqslant \kappa_1 \leqslant 1$, $\kappa_2 = 1 - \kappa_1$, and $\boldsymbol{\phi} = (\boldsymbol{\phi}_1, \boldsymbol{\phi}_2)$ on Ω, we denote

$$\{\boldsymbol{\sigma}(\boldsymbol{\phi}) \cdot \boldsymbol{n}\} := \kappa_1 \boldsymbol{\sigma}_1(\boldsymbol{\phi}_1) \cdot \boldsymbol{n} + \kappa_2 \boldsymbol{\sigma}_2(\boldsymbol{\phi}_2) \cdot \boldsymbol{n} \quad \text{at } \Gamma. \tag{4}$$

The proposed method reads: Find $\boldsymbol{U} \in V^h$ such that

$$a_{\boldsymbol{S}_h}(\boldsymbol{U}, \boldsymbol{\phi}) = L(\boldsymbol{\phi}), \quad \forall \boldsymbol{\phi} \in V^h, \tag{5}$$

where

$$\begin{aligned} a_{\boldsymbol{S}_h}(\boldsymbol{U}, \boldsymbol{\phi}) :=& (\boldsymbol{\sigma}(\boldsymbol{U}), \boldsymbol{\varepsilon}(\boldsymbol{\phi}))_{\Omega_1 \cup \Omega_2} - ((\boldsymbol{I} - \boldsymbol{S}_h \boldsymbol{K})\{\boldsymbol{n} \cdot \boldsymbol{\sigma}(\boldsymbol{U})\}, [\boldsymbol{\phi}])_\Gamma - ((\boldsymbol{I} - \boldsymbol{S}_h \boldsymbol{K})[\boldsymbol{U}], \{\boldsymbol{n} \cdot \boldsymbol{\sigma}(\boldsymbol{\phi})\})_\Gamma \\ & - (\boldsymbol{K}(\boldsymbol{I} - \boldsymbol{S}_h \boldsymbol{K})\{\boldsymbol{n} \cdot \boldsymbol{\sigma}(\boldsymbol{U})\}, \{\boldsymbol{n} \cdot \boldsymbol{\sigma}(\boldsymbol{\phi})\})_\Gamma + (\boldsymbol{S}_h([\boldsymbol{U}], [\boldsymbol{\phi}]))_\Gamma. \end{aligned} \tag{6}$$

Here $\boldsymbol{S}_h$ is a matrix which depends on the interface conditions of the problem, the local meshsize, and a penalty parameter δ which has to be large enough for the method to be stable (see Theorem 1). More precisely, on an element K with with diameter h_K,

$$\boldsymbol{S}_h|_K = (h_K/\delta + \boldsymbol{K})^{-1}.$$

To guarantee stability of this method using elements with *internal* discontinuities, further conditions on the combinations of numerical stresses must be imposed by choosing appropriate mesh and geometry

dependent weights κ. For any element K, let $K_i = K \cap \Omega_i$ denote the part of K in Ω_i. We now choose the numerical stresses in our method by

$$\kappa_1|_K = \begin{cases} 1 & \text{if } |K_1| \geqslant |K_2|, \\ 0 & \text{if } |K_1| < |K_2|, \end{cases} \quad \text{and} \quad \kappa_2 = |1 - \kappa_1|, \tag{7}$$

where $|K|$ denotes the size (area or volume) of K. The numerical stresses on the interface are then defined by (4). Thus, for an intersected element, we compute the numerical stress at that side of the interface where the larger part of the element resides. When an element side is entirely contained in the interface, one may indeed chose any convex combination of the stresses on each side.

We remark that the form $a_{\boldsymbol{S}_h}(\cdot,\cdot)$ formally coincides with $a_{\boldsymbol{S}}(\cdot,\cdot)$ in the limit case $\boldsymbol{S}_h = \boldsymbol{K}^{-1}$ corresponding to $h_K = 0$. Note also that, in the case $\boldsymbol{K} = 0$, $a_{\boldsymbol{S}_h}(\cdot,\cdot)$ coincides with the standard Nitsche form used in [4]. Thus the proposed method extends these methods into one single method for all compliancy parameters $\alpha \geqslant 0$, $\beta \geqslant 0$.

Note that the method so defined is semi-discrete in the sense that we assume exact integration on domains of all integrals in the discrete form. The domains of integration may be curved or have curved boundaries. In our implementation in 2D, however, the curved parts of the interface are replaced by straight lines on each element.

A bilinear form related to $a_{\boldsymbol{S}_h}$ has been used for the purpose of curved boundary approximation by Bramble et al. [3].

3.2.1. Mesh assumptions

We will use the following notation for mesh related quantities. Let h_K be the diameter of K and $h_{\max} = \max_{K \in T_h} h_K$. By $G_h := \{K \in T_h : K \cap \Gamma \neq \emptyset\}$ we denote the set of elements that are intersected by the interface. For an element $K \in G_h$, let $\Gamma_K := \Gamma \cap K$ be the part of Γ in K. By $h := h(\boldsymbol{x})$ we denote the piecewise discontinuous function that fulfills $h|_K = h_K$.

We make the following assumptions regarding the mesh and the interface, here formulated for the case of three dimensions. For the case of 2D, see [4].

A1: The triangulation is non-degenerate, i.e.,

$$h_K/\rho_K \leqslant C \quad \forall K \in T_h,$$

where h_K is the diameter of K and ρ_K is the diameter of the largest ball contained in K.

A2: The intersection of Γ and the boundary of $K \in G_h$ is either a connected curve, or else a side of K. (The first case implies that Γ divides each $K \in G_h$ into two parts and intersects three or four edges of K in one point each.)

A3: For the first case in A2, take a plane through three of the points of intersection between Γ and the edges of K, and let $\Gamma_{K,h}$ be the intersection between K and this plane. Then Γ_K is a function on $\Gamma_{K,h}$ for some choice of points of intersection; thus

$$\Gamma_K = \{(\xi,\eta,\zeta) : (\xi,\eta,0) \in \Gamma_{K,h}, \zeta = g(\xi,\eta)\}$$

in local coordinates (ξ,η,ζ).

Assumption A1 is standard. Further, since the curvature of Γ is bounded, A2 and A3 are fulfilled on *some* sufficiently fine mesh. In view of this fact, we may think of A3 as expressing that the curvature of the interface is well resolved by the mesh. A2 and A3 are chosen with the purpose to ensure that the convergence analysis of the method does not become too complicated. The method may indeed be formulated and analyzed under somewhat less restrictive mesh conditions, e.g., conditions that allow for more general intersections of an element boundary ∂K and Γ than in assumption A2. We shall not pursue these issues

when it comes to the theoretical properties of our method, but restrict ourselves to the case when assumptions A1–A3 hold.

4. A priori error analysis

In this section, we shall prove the convergence result in Theorem 1 below. Recall that G_h denotes the set of elements that are intersected by the interface. We will use the mesh dependent norms

$$\|\boldsymbol{v}\|_{1/2,h,\Gamma}^2 := \sum_{K\in G_h} h_K^{-1}\|\boldsymbol{v}\|_{0,\Gamma_K}^2,$$

$$\|\boldsymbol{v}\|_{-1/2,h,\Gamma}^2 := \sum_{K\in G_h} h_K\|\boldsymbol{v}\|_{0,\Gamma_K}^2,$$

and the energy type norm

$$|||\boldsymbol{v}|||^2 := (\boldsymbol{\sigma}(\boldsymbol{v}),\boldsymbol{\varepsilon}(\boldsymbol{v}))_{\Omega_1\cup\Omega_2} + \|\boldsymbol{S}_h^{1/2}[\boldsymbol{v}]\|_{0,\Gamma}^2 + \delta^{-1}\|\{\boldsymbol{\sigma}(\boldsymbol{v})\}\cdot\boldsymbol{n}\|_{-1/2,h,\Gamma}^2.$$

Our main result reads as follows.

Theorem 1. *Under assumptions A1–A3 of Section* 3, *and for* $\boldsymbol{u}$ *solving* (5) *and* $\boldsymbol{U}$ *solving* (5), *the following a priori error estimate holds. If the penalty parameter* δ *is large enough, then*

$$|||\boldsymbol{u}-\boldsymbol{U}||| \leqslant Ch_{\max}\|\boldsymbol{u}\|_{2,\Omega_1\cup\Omega_2}. \tag{8}$$

The choice $\delta = 8C_I(2\mu_m + 3\lambda_m)$ *is sufficient. Here* $\lambda_m := \max_\Omega \lambda$, $\mu_m := \max_\Omega \mu$, *and* C_I *is a constant depending only on the degree of non-degeneracy of the mesh and the curvature of* Γ, *see Lemma* 6 *below. Moreover, the convergence is uniform with respect to the compliancy of the interface, i.e., the error constants in* 8 *and* 22 *are independent of* α *and* β.

The proof of this theorem requires several lemmas. We start by collecting some elementary properties of the penalty matrix $\boldsymbol{S}_h$.

Lemma 2. *Let* $\boldsymbol{S}_h := (h/\delta + \boldsymbol{K})^{-1}$, *and let* $|\cdot|$ *denote the matrix norm induced by the Euclidean norm on* $\mathbb{R}^n$. *Then*

$$\boldsymbol{I} - \boldsymbol{S}_h\boldsymbol{K} = \frac{h}{\delta}\boldsymbol{S}_h, \tag{9}$$

$$|\boldsymbol{S}_h| \leqslant \frac{\delta}{h}, \tag{10}$$

$$|\boldsymbol{I} - \boldsymbol{S}_h\boldsymbol{K}| \leqslant 1, \tag{11}$$

and

$$|\boldsymbol{K}(\boldsymbol{I} - \boldsymbol{S}_h\boldsymbol{K})| \leqslant \frac{h}{\delta}. \tag{12}$$

Proof. The first identity is obvious. As $\boldsymbol{K}$ is positive definite, (10) follows from the definition of $\boldsymbol{S}_h$, and (11) follows from (9) and (10). Writing

$$\boldsymbol{K}(\boldsymbol{I}-\boldsymbol{S}_h\boldsymbol{K}) = \boldsymbol{K}\frac{h}{\delta}\boldsymbol{S}_h = \frac{h}{\delta}\left(\boldsymbol{K}+\frac{h}{\delta}-\frac{h}{\delta}\right)\boldsymbol{S}_h = \frac{h}{\delta}\left(\boldsymbol{I}-\frac{h}{\delta}\boldsymbol{S}_h\right),$$

we see that since $\boldsymbol{S}_h$ is positive definite, (12) follows from (10). □

4.1. Approximation properties of V^h

We further need a variant of the well known trace inequality

$$\|w\|^2_{0,\partial\tilde{K}} \leqslant C\|w\|_{0,\tilde{K}}\|w\|_{1,\tilde{K}}, \quad \forall w \in H^1(\tilde{K}), \tag{13}$$

on a reference element $\tilde{K}$. The crucial fact in Lemma 3 is that the constant in (14) is independent of the location of the interface relative to the mesh. We give here a proof of this Lemma which is simpler than the proof in [4].

Lemma 3. *Map a tetrahedron $K \in G_h$ onto the unit reference tetrahedron $\tilde{K}$ by an affine map and denote by $\tilde{\Gamma}_{\tilde{K}}$ the corresponding image of Γ_K. Under assumptions A1–A3 of Section 3 there exist a constant C, depending on Γ but independent of the mesh, such that*

$$\|w\|^2_{0,\tilde{\Gamma}_{\tilde{K}}} \leqslant C\|w\|_{0,\tilde{K}}\|w\|_{1,\tilde{K}}, \quad \forall w \in H^1(\tilde{K}). \tag{14}$$

Proof. Recall that, by assumption A3,

$$\Gamma_K = \{(\xi,\eta,\zeta) : (\xi,\eta,0) \in \Gamma_{K,h}, \zeta = g(\xi,\eta)\}.$$

On the reference element we may write, using again (ξ,η,ζ) to denote local coordinates on $\tilde{K}$,

$$\tilde{\Gamma}_{\tilde{K}} = \{(\xi,\eta,\zeta) : (\xi,\eta,0) \in \tilde{\Gamma}_{\tilde{K},h}, \zeta = \tilde{g}(\xi,\eta)\}.$$

We let $\mathbf{n}$ denote the outward unit normal of $\tilde{K}_1$ and note that for its component in the ζ-direction we have $n_\zeta = \pm(1+|\nabla\tilde{g}|^2)^{-1/2}$ on $\tilde{\Gamma}$. By the divergence theorem,

$$\begin{aligned} 2\int_{\tilde{K}_i} w\frac{\partial w}{\partial\zeta}\,\mathrm{d}V &= \int_{\tilde{K}_i}\operatorname{div}(0,0,w^2)\,\mathrm{d}V = \int_{\partial\tilde{K}_i}\boldsymbol{n}\cdot(0,0,w^2)\,\mathrm{d}A \\ &= \int_{\tilde{\Gamma}_{\tilde{K}}} w^2(1+|\nabla\tilde{g}|^2)^{-1/2}\,\mathrm{d}A + \int_{\partial\tilde{K}_1\setminus\tilde{\Gamma}_{\tilde{K}}} n_\zeta w^2\,\mathrm{d}A. \end{aligned} \tag{15}$$

Since the interface is smooth and bounded and the mesh is non-degenerate, $|\frac{\partial g}{\partial\xi}|^2 + |\frac{\partial g}{\partial\eta}|^2 \leqslant Ch_K^2$, and thus $|\nabla\tilde{g}| \leqslant C$, which implies that

$$\|w\|^2_{0,\tilde{\Gamma}_{\tilde{K}}} \leqslant C\int_{\tilde{\Gamma}_{\tilde{K}}} w^2(1+|\nabla\tilde{g}|^2)^{-1/2}\,\mathrm{d}A.$$

By (15) we thus find, using Cauchy–Schwarz' inequality, that

$$\|w\|^2_{0,\tilde{\Gamma}_{\tilde{K}}} \leqslant C(\|w\|_{0,\widetilde{K_1}}\|w\|_{1,\widetilde{K_1}} + \|w\|^2_{0,\partial\tilde{K}_1\setminus\tilde{\Gamma}_{\tilde{K}}}).$$

The result of the lemma now follows from (13). □

To show that functions in V^h approximate functions $\boldsymbol{v} \in [H^1_0(\Omega)]^n \cap [H^2(\Omega_1\cup\Omega_2)^n]$ to the order h in the norm $|||\cdot|||$, we construct an interpolant of $\boldsymbol{v}$ by nodal interpolants of $[H^2]^n$-extensions of $\boldsymbol{v}_1$ and $\boldsymbol{v}_2$ as follows. Choose extensions operators $\mathsf{E}_i : [H^2(\Omega_i)]^n \to [H^2(\Omega)]^n$ such that $(\mathsf{E}_i\boldsymbol{w})|_{\Omega_i} = \boldsymbol{w}$ and

$$\|\mathsf{E}_i \boldsymbol{w}\|_{s,\Omega} \leqslant C\|\boldsymbol{w}\|_{s,\Omega_i} \quad \forall \boldsymbol{w} \in [H^s(\Omega_i)]^n, \quad s = 0, 1, 2. \tag{16}$$

Let I_h be the standard Lagrangian nodal interpolation operator and define

$$I_h^* \boldsymbol{v} := (I_{h,1}^* \boldsymbol{v}_1, I_{h,2}^* \boldsymbol{v}_2) \quad \text{where } I_{h,i}^* \boldsymbol{v}_i := (I_h \mathsf{E}_i \boldsymbol{v}_i)|_{\Omega_i}. \tag{17}$$

The following theorem is valid.

Theorem 4. *Let I_h^* be an interpolation operator defined as in* (17). *Then for $\boldsymbol{v} \in [H_0^1(\Omega)]^n \cap [H^2(\Omega_1 \cup \Omega_2)]^n$*

$$|||\boldsymbol{v} - I_h^* \boldsymbol{v}||| \leqslant C_A \max(\delta^{-1/2}, \delta^{1/2}) h_{\max} \|\boldsymbol{v}\|_{2,\Omega_1 \cup \Omega_2}.$$

Proof. In the same way as in [4], Theorem 2, it follows from Lemma 3 that with

$$\|\boldsymbol{v}\|_h^2 := (\boldsymbol{\sigma}(\boldsymbol{v}), \boldsymbol{\varepsilon}(\boldsymbol{v}))_{\Omega_1 \cup \Omega_2} + \|[\boldsymbol{v}]\|_{1/2,h,\Gamma}^2 + \|\{\boldsymbol{\sigma}(\boldsymbol{v})\} \cdot \boldsymbol{n}\|_{-1/2,h,\Gamma}^2$$

there holds

$$\|\boldsymbol{v} - I_h^* \boldsymbol{v}\|_h \leqslant C_A h_{\max} \|\boldsymbol{v}\|_{2,\Omega_1 \cup \Omega_2}, \quad \forall \boldsymbol{v} \in [H_0^1(\Omega)]^n \cap [H^2(\Omega_1 \cup \Omega_2)]^n.$$

Here the approximation constant C_A does not depend on the complicancy parameters α and β, nor on the location of the interface relative to the mesh. It follows from (10) that

$$\|\boldsymbol{S}_h^{1/2}[\boldsymbol{v} - I_h^* \boldsymbol{v}]\|_{0,\Gamma}^2 \leqslant \delta \|[\boldsymbol{v} - I_h^* \boldsymbol{v}]\|_{1/2,h,\Gamma}^2,$$

whence

$$|||\boldsymbol{v} - I_h^* \boldsymbol{v}|||^2 \leqslant \max(\delta^{-1}, \delta) \|\boldsymbol{v} - I_h^* \boldsymbol{v}\|_h^2$$

and the result follows. □

4.2. Stability and convergence

The following consistency relation follows directly by use of Green's formula.

Lemma 5. *The discrete problem* (5) *is consistent in the sense that, for $\boldsymbol{u}$ solving* (1),

$$a_{S_h}(\boldsymbol{u}, \boldsymbol{\phi}) = L(\boldsymbol{\phi}), \quad \forall \boldsymbol{\phi} \in V^h.$$

An immediate consequence of Lemma 5 is the orthogonality condition

$$a_{S_h}(\boldsymbol{u} - \boldsymbol{U}, \boldsymbol{\phi}) = 0, \quad \forall \boldsymbol{\phi} \in V^h. \tag{18}$$

In order to show that the bilinear form $a_{S_h}(\cdot, \cdot)$ is coercive on V^h, we need the following inverse inequality.

Lemma 6. *For $\boldsymbol{\phi} \in V^h$, the following inverse inequality holds*:

$$\|\{\boldsymbol{\sigma}(\boldsymbol{\phi})\}\|_{-1/2,h,\Gamma}^2 \leqslant C_I \|\boldsymbol{\sigma}(\boldsymbol{\phi})\|_{0,\Omega_1 \cup \Omega_2}^2.$$

Proof. Assume without restriction that $|K_1| \geqslant |K_2|$ so that $\kappa_1 = 1$ and $\kappa_2 = 0$. Since $\boldsymbol{\phi} \in V^h$ is linear on K_1, $\boldsymbol{\sigma}(\boldsymbol{\phi}_1)$ is constant and we have

$$h_K\|\kappa_1\boldsymbol{\sigma}_1(\boldsymbol{\phi}_1)\|^2_{0,\Gamma_K} = h_K|\Gamma_K||\boldsymbol{\sigma}_1(\boldsymbol{\phi}_1)|^2 = h_K\frac{|\Gamma_K|}{|K_1|}\|\boldsymbol{\sigma}_1(\boldsymbol{\phi}_1)\|^2_{0,K_1} \leqslant C\|\boldsymbol{\sigma}_1(\boldsymbol{\phi}_1)\|^2_{0,K_1}.$$

In the last step above we have used that, since the curvature of Γ is bounded, $|\Gamma_K| \leqslant Ch_K$, and, since the mesh is non-degenerate, $|K_1| \geqslant |K|/2 \geqslant ch_K^2$. The result follows by summation over the elements. □

Lemma 7. *The discrete form $a_{\boldsymbol{S}_h}(\cdot,\cdot)$ is continuous, i.e.,*

$$a_{\boldsymbol{S}_h}(\boldsymbol{u},\boldsymbol{v}) \leqslant C_C|||\boldsymbol{u}||| \; |||\boldsymbol{v}||| \quad \forall \boldsymbol{u},\boldsymbol{v} \in V \cup V^h.$$

Further, it is coercive on V^h w.r.t. $|||\cdot|||$, i.e., if $\delta \geqslant 8C_I(2\mu_m + 3\lambda_m)$ then

$$a_{\boldsymbol{S}_h}(\boldsymbol{v},\boldsymbol{v}) \geqslant \frac{1}{2}|||\boldsymbol{v}|||^2 \quad \forall \boldsymbol{v} \in V^h.$$

Proof. To show continuity, we note that by (9) and (11)

$$|((\boldsymbol{I} - \boldsymbol{S}_h\boldsymbol{K})\boldsymbol{u},\boldsymbol{v})_\Gamma| = \delta^{-1/2}|((\boldsymbol{I} - \boldsymbol{S}_h\boldsymbol{K})^{1/2}h^{1/2}\boldsymbol{u}, \boldsymbol{S}_h^{1/2}\boldsymbol{v})_\Gamma| \leqslant \delta^{-1/2}\int_\Gamma h^{1/2}|\boldsymbol{u}\cdot\boldsymbol{S}_h^{1/2}\boldsymbol{v}|\,\mathrm{d}\sigma. \tag{19}$$

Thus the second term in the definition (6) of $a_{\boldsymbol{S}_h}$ is bounded as follows:

$$|((\boldsymbol{I} - \boldsymbol{S}_h\boldsymbol{K})\{\boldsymbol{n}\cdot\boldsymbol{\sigma}(\boldsymbol{u})\},[\boldsymbol{v}])_\Gamma| \leqslant \frac{1}{\delta^{1/2}}\|\{\boldsymbol{n}\cdot\boldsymbol{\sigma}(\boldsymbol{u})\}\|_{-1/2,h,\Gamma}\|\boldsymbol{S}_h^{1/2}[\boldsymbol{v}]\|_{0,\Gamma},$$

and an appropriate bound for the third term is obtained in the same way. For the fourth term we use (12) and find that

$$|(\boldsymbol{K}(\boldsymbol{I} - \boldsymbol{S}_h\boldsymbol{K})\{\boldsymbol{n}\cdot\boldsymbol{\sigma}(\boldsymbol{u})\},\{\boldsymbol{n}\cdot\boldsymbol{\sigma}(\boldsymbol{v})\})_\Gamma| \leqslant \frac{1}{\delta}\|\{\boldsymbol{n}\cdot\boldsymbol{\sigma}(\boldsymbol{u})\}\|_{-1/2,h,\Gamma}\|\{\boldsymbol{n}\cdot\boldsymbol{\sigma}(\boldsymbol{v})\}\|_{-1/2,h,\Gamma}.$$

Using these estimates together with obvious bounds for the remaining terms in (6), continuity of $a_{\boldsymbol{S}_h}$ follows. Here the constant C_C does not depend on the problem parameters, nor on δ.

To show coercivity, we first note that the stress–strain relation can be inverted to yield

$$\boldsymbol{\varepsilon} = \frac{1}{2\mu}\left(\boldsymbol{\sigma} - \frac{\lambda}{3\lambda+2\mu}\mathrm{tr}\,\boldsymbol{\sigma}\boldsymbol{I}\right) = \frac{1}{2\mu}\boldsymbol{\sigma}^D + \frac{1}{9\lambda+6\mu}\mathrm{tr}\,\boldsymbol{\sigma}\boldsymbol{I},$$

where $\boldsymbol{\sigma}^D := \boldsymbol{\sigma} - \mathrm{tr}\,\boldsymbol{\sigma}\boldsymbol{I}/3$ and $\mathrm{tr}\,\boldsymbol{\sigma} := \sum_i \sigma^{ii}$, and thus we have that

$$\boldsymbol{\sigma} : \boldsymbol{\varepsilon} = \frac{1}{2\mu}\boldsymbol{\sigma}^D : \boldsymbol{\sigma}^D + \frac{1}{9\lambda+6\mu}(\mathrm{tr}\,\boldsymbol{\sigma})^2,$$

and

$$\boldsymbol{\sigma} : \boldsymbol{\sigma} = \boldsymbol{\sigma}^D : \boldsymbol{\sigma}^D + \frac{1}{3}(\mathrm{tr}\,\boldsymbol{\sigma})^2,$$

so that

$$\boldsymbol{\sigma} : \boldsymbol{\sigma} \leqslant (2\mu + 3\lambda)\boldsymbol{\sigma} : \boldsymbol{\varepsilon}. \tag{20}$$

By definition of $a_{\boldsymbol{S}_h}(\cdot,\cdot)$, we have

$$\begin{aligned} a_{\boldsymbol{S}_h}(\boldsymbol{v},\boldsymbol{v}) = {} & (\boldsymbol{\sigma}(\boldsymbol{v}),\boldsymbol{\varepsilon}(\boldsymbol{v}))_{\Omega_1\cup\Omega_2} - 2((\boldsymbol{I} - \boldsymbol{S}_h\boldsymbol{K})\{\boldsymbol{n}\cdot\boldsymbol{\sigma}(\boldsymbol{v})\},[\boldsymbol{v}])_\Gamma \\ & - (\boldsymbol{K}(\boldsymbol{I} - \boldsymbol{S}_h\boldsymbol{K})\{\boldsymbol{n}\cdot\boldsymbol{\sigma}(\boldsymbol{v})\},\{\boldsymbol{n}\cdot\boldsymbol{\sigma}(\boldsymbol{v})\})_\Gamma + (\boldsymbol{S}_h[\boldsymbol{v}],[\boldsymbol{v}])_\Gamma. \end{aligned} \tag{21}$$

We consider first the second term on the right and note that by (19)

$$\begin{aligned}2((\boldsymbol{I}-\boldsymbol{S}_h\boldsymbol{K})\{\boldsymbol{n}\cdot\boldsymbol{\sigma}(\boldsymbol{v})\},[\boldsymbol{v}])_\Gamma &\leqslant 2(\sqrt{h/\delta}\{\boldsymbol{n}\cdot\boldsymbol{\sigma}(\boldsymbol{v})\},\boldsymbol{S}_h^{1/2}[\boldsymbol{v}])_\Gamma\\ &\leqslant \frac{2}{\sqrt{\delta}}\|\{\boldsymbol{n}\cdot\boldsymbol{\sigma}(\boldsymbol{v})\}\|_{-1/2,h,\Gamma}\|\boldsymbol{S}_h^{1/2}[\boldsymbol{v}]\|_{0,\Gamma}\\ &\leqslant \frac{2}{\delta}\|\{\boldsymbol{n}\cdot\boldsymbol{\sigma}(\boldsymbol{v})\}\|^2_{-1/2,h,\Gamma}+\frac{1}{2}\|\boldsymbol{S}_h^{1/2}[\boldsymbol{v}]\|^2_{0,\Gamma}.\end{aligned}$$

To bound the first term on the right we apply Lemma 6 and (20). We obtain that

$$2((\boldsymbol{I}-\boldsymbol{S}_h\boldsymbol{K})\{\boldsymbol{n}\cdot\boldsymbol{\sigma}(\boldsymbol{v})\},[\boldsymbol{v}])_\Gamma\leqslant\frac{2}{\delta}C_I(2\mu_m+3\lambda_{\mathrm{m}})(\boldsymbol{\sigma}(\boldsymbol{v}),\boldsymbol{\varepsilon}(\boldsymbol{v}))_{0,\Omega_1\cup\Omega_2}+\frac{1}{2}\|\boldsymbol{S}_h^{1/2}[\boldsymbol{v}]\|^2_{0,\Gamma},$$

where $\lambda_m:=\max_\Omega\lambda$ and $\mu_m:=\max_\Omega\mu$. For the third term, we have, using (12), Lemma 6, and (20),

$$(\boldsymbol{K}(\boldsymbol{I}-\boldsymbol{S}_h\boldsymbol{K})\{\boldsymbol{n}\cdot\boldsymbol{\sigma}(\boldsymbol{v})\},\{\boldsymbol{n}\cdot\boldsymbol{\sigma}(\boldsymbol{v})\})_\Gamma\leqslant\frac{1}{\delta}\|\{\boldsymbol{n}\cdot\boldsymbol{\sigma}(\boldsymbol{v})\}\|^2_{-1/2,h,\Gamma}\leqslant\frac{1}{\delta}C_I(2\mu_m+3\lambda_m)(\boldsymbol{\sigma}(\boldsymbol{v}),\boldsymbol{\varepsilon}(\boldsymbol{v}))_{0,\Omega_1\cup\Omega_2}.$$

Applying these bounds in (21) and collecting the terms we find that

$$a_{\boldsymbol{S}_h}(\boldsymbol{v},\boldsymbol{v})\geqslant\left(1-\frac{3}{\delta}C_I(2\mu_m+3\lambda_m)\right)(\boldsymbol{\sigma}(\boldsymbol{v}),\boldsymbol{\varepsilon}(\boldsymbol{v}))_{\Omega_1\cup\Omega_2}+\left(1-\frac{1}{2}\right)\|\boldsymbol{S}_h^{1/2}[\boldsymbol{v}]\|^2_{0,\Gamma}.$$

Adding and subtracting $\delta^{-1}\|\{\boldsymbol{n}\cdot\boldsymbol{\sigma}(\boldsymbol{v})\}\|^2_{-1/2,h,\Gamma}$ and using again Lemma 6 and (20) we arrive at

$$a_{\boldsymbol{S}_h}(\boldsymbol{v},\boldsymbol{v})\geqslant\left(1-\frac{4}{\delta}C_I(2\mu_{\mathrm{m}}+3\lambda_{\mathrm{m}})\right)(\boldsymbol{\sigma}(\boldsymbol{v}),\boldsymbol{\varepsilon}(\boldsymbol{v}))_{\Omega_1\cup\Omega_2}+\frac{1}{\delta}\|\{\boldsymbol{n}\cdot\boldsymbol{\sigma}(\boldsymbol{v})\}\|^2_{-1/2,h,\Gamma}+\frac{1}{2}\|\boldsymbol{S}_h^{1/2}[\boldsymbol{v}]\|^2_{0,\Gamma}.$$

This concludes the proof since $\delta\geqslant 8C_I(2\mu_m+3\lambda_m)$. □

We are now ready for the

Proof of Theorem 1. By Lemma 7 and orthogonality, we have that

$$|||\boldsymbol{U}-\boldsymbol{v}|||^2\leqslant 2a_{\boldsymbol{S}_h}(\boldsymbol{U}-\boldsymbol{v},\boldsymbol{U}-\boldsymbol{v})=2a_{\boldsymbol{S}_h}(\boldsymbol{u}-\boldsymbol{v},\boldsymbol{U}-\boldsymbol{v})\leqslant 2C_C|||\boldsymbol{u}-\boldsymbol{v}|||\;|||\boldsymbol{U}-\boldsymbol{v}|||,$$

and it follows that

$$|||\boldsymbol{u}-\boldsymbol{U}|||\leqslant 2C_C|||\boldsymbol{u}-\boldsymbol{v}|||\quad\forall\boldsymbol{v}\in V^h.$$

Taking $\boldsymbol{v}=I_h^*\boldsymbol{u}$ and invoking the interpolation result of Theorem 4, (8) follows. □

We conclude this section by showing second order convergence of the L_2-norm of the error.

Theorem 8. *Under the assumptions of Theorem* 1, *there holds*

$$\|\boldsymbol{u}-\boldsymbol{U}\|_{0,\Omega}\leqslant Ch^2_{\max}\|\boldsymbol{u}\|_{2,\Omega_1\cup\Omega_2}. \tag{22}$$

Proof. The proof is standard, using a duality argument. Define $\boldsymbol{z}=(\boldsymbol{z}_1,\boldsymbol{z}_2)$ by

$$\begin{aligned}&-\nabla\cdot\boldsymbol{\sigma}(\boldsymbol{z})=\boldsymbol{e}\quad\text{in }\Omega_1\cup\Omega_2,\\ &\boldsymbol{z}_i=0\quad\text{on }\partial\Omega\cap\partial\Omega_i,\\ &[\boldsymbol{\sigma}(\boldsymbol{z})\cdot\boldsymbol{n}]=0\quad\text{on }\Gamma,\\ &[\boldsymbol{z}]+\boldsymbol{K}\boldsymbol{\sigma}(\boldsymbol{z})\cdot\boldsymbol{n}=0\quad\text{on }\Gamma.\end{aligned} \tag{23}$$

where $\boldsymbol{\sigma}(\boldsymbol{z}) := 2\mu\boldsymbol{\varepsilon}(\boldsymbol{z}) + \lambda\nabla\cdot\boldsymbol{z}\boldsymbol{I}$ and $\boldsymbol{e} := \boldsymbol{u} - \boldsymbol{U}$. By Green's formula we have that

$$\begin{aligned}\|\boldsymbol{e}\|_{0,\Omega}^2 &= -(\nabla\cdot\boldsymbol{\sigma}(\boldsymbol{z}),\boldsymbol{e})_{\Omega_1\cup\Omega_2} = (\boldsymbol{\sigma}(\boldsymbol{z}),\boldsymbol{\varepsilon}(\boldsymbol{e}))_\Omega - (\boldsymbol{\sigma}(\boldsymbol{z}_1)\cdot\boldsymbol{n},\boldsymbol{e}_1) + (\boldsymbol{\sigma}(\boldsymbol{z}_2)\cdot\boldsymbol{n},\boldsymbol{e}_2)\\ &= (\boldsymbol{\sigma}(\boldsymbol{z}),\boldsymbol{\varepsilon}(\boldsymbol{e}))_\Omega - (\{\boldsymbol{\sigma}(\boldsymbol{z})\cdot\boldsymbol{n}\},[\boldsymbol{e}])_\Gamma = a_{S_h}(\boldsymbol{z},\boldsymbol{e}),\end{aligned}$$

since $[\boldsymbol{z}] + \boldsymbol{K}\{\boldsymbol{\sigma}(\boldsymbol{z})\cdot\boldsymbol{n}\} = 0$. Thus, using the symmetry of $a_{S_h}(\cdot,\cdot)$ and applying the orthogonality relation (18) and Theorem 4, we find that

$$\|\boldsymbol{e}\|_{0,\Omega}^2 = a_{S_h}(\boldsymbol{z} - I_h\boldsymbol{z},\boldsymbol{e}) \leqslant C|||\boldsymbol{z} - I_h\boldsymbol{z}|||\ |||\boldsymbol{e}||| \leqslant Ch_{\max}\|\boldsymbol{z}\|_{2,\Omega_1\cup\Omega_2}|||\boldsymbol{e}|||. \tag{24}$$

Finally, by elliptic regularity, cf. [6], we have $\|\boldsymbol{z}\|_{2,\Omega_1\cup\Omega_2} \leqslant C\|\boldsymbol{e}\|_{0,\Omega}$, with dependence on the material data in the constant, whence the estimate (22) follows from (24) and (8). □

5. Numerical examples

In this section, we give some numerical examples of the capabilities and behaviour of our approach. We start giving an example of a linear problems with smooth solution, where the optimal order convergence of the proposed method is confirmed.

In order to demonstrate the applicability of our approach to more general problems—i.e., problems which are not covered by the theoretical analysis above—we shall further consider an elastic contact problem and a simple crack propagation model with hardening at the interface.

The basic implementation issues in this method were discussed above and further in [4]. Below we shall give some additional details concerning the implementation of the contact and crack propagation problems. For computational convenience, we make the following simplification: in all cases, the interface is approximated in the element interiors using linear interpolation between the points marking the intersection between the interface and the element edges.

5.1. Convergence test for a linear problem

In order to confirm the convergence of our method in a case where the theoretical convergence analysis applies, we have considered an inclusion problem with exact solution from Sukumar et al. [8]. The problem is radially symmetric with different material properties in concentric discs around the origin. The inner disc has material parameters E_1, ν_1, and the outer E_2, ν_2. At any point, the displacement vector can be written $\boldsymbol{u} = (u^r, u^\theta)$, where u^r is the radial component of the displacement and u^θ is the circumferential component. The material is subjected to a boundary displacement $\boldsymbol{u} = \boldsymbol{x}$ (in Cartesian coordinates), and the exact solution to the problem is given by (cf. [8])

$$u^r(r) = \begin{cases} \left(\left(1 - \dfrac{b^2}{a^2}\right)c + \dfrac{b^2}{a^2}\right)r, & 0 \leqslant r \leqslant a,\\ \left(r - \dfrac{b^2}{r}\right)c + \dfrac{b^2}{r}, & a \leqslant r \leqslant b,\end{cases}$$

$$u^\theta = 0,$$

with

$$c = \frac{(\lambda_1 + \mu_1 + \mu_2)b^2}{(\lambda_2 + \mu_2)a^2 + (\lambda_1 + \mu_1)(b^2 - a^2) + \mu_2 b^2}.$$

We followed [8] and chose $E_1 = 1$, $\nu_1 = 0.25$, and $E_2 = 10$, $\nu_2 = 0.3$. The problem was solved on a quarter of a disc with symmetry boundary conditions on the vertical and horizontal boundaries and with the given boundary condition on the circumference.

In Fig. 1 we show the final computational mesh in a sequence, with the location of the interface at $a = 0.4$ indicated, in Fig. 2 we give the elevation of the length of the computed displacement vector, and in Fig. 3 we show the (expected) second order L_2-convergence achieved with our method.

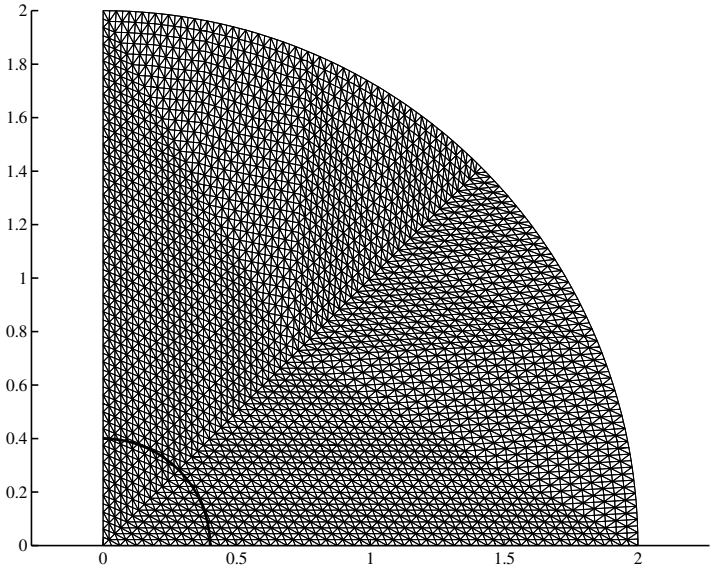

Fig. 1. Final computational mesh with the location of the interface indicated.

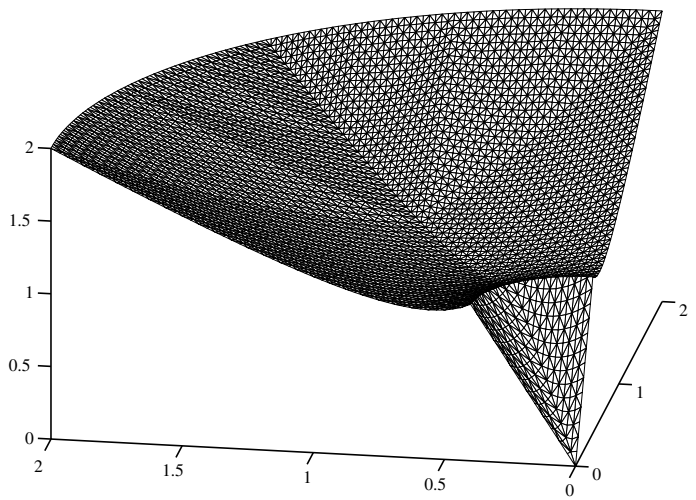

Fig. 2. Elevation of the magnitude of the computed displacement vector on the final mesh.

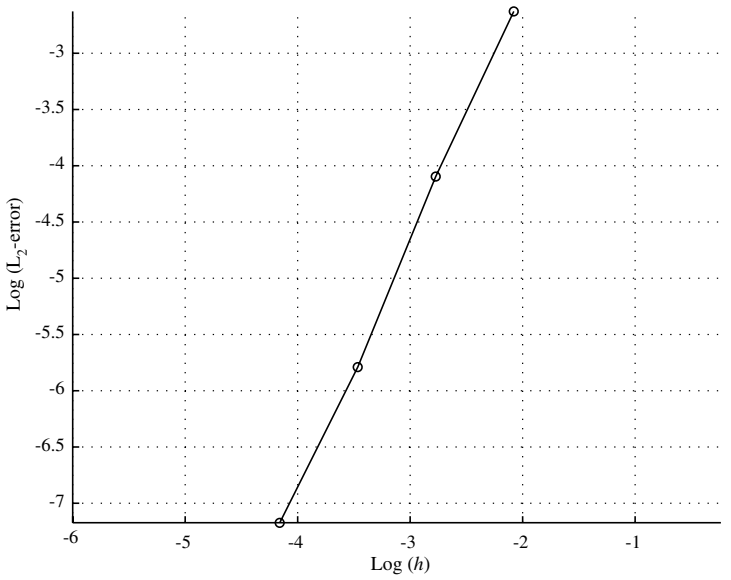

Fig. 3. Second order convergence in $L_2(\Omega)$.

5.2. Contact

We have considered the following model problem: find $\boldsymbol{u}$ and $\boldsymbol{\sigma}$ such that

$$\begin{aligned}
&\boldsymbol{\sigma} = \lambda \nabla \cdot \boldsymbol{u}\boldsymbol{I} + 2\mu\boldsymbol{\varepsilon}(\boldsymbol{u}) \quad \text{in } \Omega_1 \cup \Omega_2,\\
&-\nabla \cdot \boldsymbol{\sigma} = \boldsymbol{f} \quad \text{in } \Omega_1 \cup \Omega_2,\\
&\boldsymbol{u} = 0 \quad \text{on } \partial\Omega,\\
&[\boldsymbol{u}\cdot\boldsymbol{n}] \leqslant 0, \sigma_n \leqslant 0, \sigma_n[\boldsymbol{u}\cdot\boldsymbol{n}] = 0, \quad \boldsymbol{\sigma}_t = 0 \text{ on } \Gamma,
\end{aligned} \tag{25}$$

where $\sigma_n = \boldsymbol{n}\cdot\boldsymbol{\sigma}\cdot\boldsymbol{n}$ and $\boldsymbol{\sigma}_t = \boldsymbol{\sigma}\cdot\boldsymbol{n} - \sigma_n\boldsymbol{n}$. This corresponds to the case where the inclusion is in frictionless contact with the exterior domain, and Γ plays the role of a Signorini interface, i.e., an interface where the two domains may (or may not) come into contact. The corresponding discrete problem is to seek $\boldsymbol{U} \in V^h$ such that

$$a_c(\boldsymbol{U}, \boldsymbol{\phi}) = L(\boldsymbol{\phi}), \quad \forall \boldsymbol{\phi} \in V^h, \tag{26}$$

where

$$\begin{aligned}
a_c(\boldsymbol{U}, \boldsymbol{\phi}) := {} & (\boldsymbol{\sigma}(\boldsymbol{U}), \boldsymbol{\varepsilon}(\boldsymbol{\phi}))_{\Omega_1\cup\Omega_2} - ([\boldsymbol{U}\cdot\boldsymbol{n}], \{\boldsymbol{n}\cdot\boldsymbol{\sigma}(\boldsymbol{\phi})\cdot\boldsymbol{n}\})_{\Gamma_c} - (\{\boldsymbol{n}\cdot\boldsymbol{\sigma}(\boldsymbol{U})\cdot\boldsymbol{n}\}, [\boldsymbol{\phi}\cdot\boldsymbol{n}])_{\Gamma_c}\\
& + (\vartheta h^{-1}([\boldsymbol{U}\cdot\boldsymbol{n}]), [\boldsymbol{\phi}\cdot\boldsymbol{n}])_{\Gamma_c},
\end{aligned}$$

and $\Gamma_c = \{\boldsymbol{x} \in \Gamma : [\boldsymbol{U}(\boldsymbol{x})\cdot\boldsymbol{n}] > 0\}$. Here a_c is non-linear and resembles the linear form a_{S_h} with $\boldsymbol{K} = 0$. We can identify $\vartheta := \delta$ in Lemma 7, and thus the discrete problem can be made coercive as long as the physical problem is well-posed.

In order to realize a solution procedure for this problem, we checked after each iteration whether the discrete solution violated $[\boldsymbol{U}\cdot\boldsymbol{n}] \leqslant 0$ or not. Wherever this condition was violated we assumed that

we were at Γ_c, and elsewhere we assumed a traction-free boundary. An alternative would be to also check the sign of σ_n; this we have not done in our implementation. We used a fixed point iteration scheme which does not necessarily converge since points in contact at one iteration may not be in contact in the next (a common problem in contact computations). Thus we stopped the iterations when the difference between two consecutive solutions were three orders of magnitude smaller than the solution after the first iteration.

For our numerical example shown in Fig. 4, we considered a domain $(0,1/2)\times(0,1)$, with $u^x = 0$ at $x = 0$, $\boldsymbol{u} = \boldsymbol{0}$ at $y = 0$, and $\boldsymbol{u} = (0,-0.1)$ at $y = 1$. In this domain, we considered a circular inclusion with higher stiffness than the surrounding material. The elasticity parameters were chosen as $v = 0.3$, $E_{\min} = 10^6$ (modulus of elasticity of the surrounding material), $E_{\max} = 10^7$ (modulus of elasticity of the inclusion). Finally, we used $\vartheta = 10E_{\max}$.

5.3. Crack propagation

We have also considered a simple rigid-hardening model for crack formation. We define $\sigma_{\max}$ as the maximum positive eigenvalue of the matrix $\sigma^{ij}(\boldsymbol{u})$ of the components of $\boldsymbol{\sigma}(\boldsymbol{u})$ and assume that as long as $\sigma_{\max} < \sigma_c$, where σ_c is a threshold value, we have $[\boldsymbol{u}] = 0$ at the crack tip. When $\sigma_{\max} \geqslant \sigma_c$, the crack (defining Γ) is assumed to run perpendicularly to the eigenvector associated with $\sigma_{\max}$ and the constitutive relation changes to $[\boldsymbol{u}] = -\boldsymbol{K}\{\boldsymbol{\sigma}(\boldsymbol{u})\cdot\boldsymbol{n}\}$. The physical problem modeled by these constitutive relations is a solid that can withstand high compression but cracks in high tension and which retains a certain stiffness in the crack zone even after crack opening. We choose this model for its simplicity; obviously, the computational framework allows for more physically realistic models. We remark that Γ changes during the computation, so again we have a non-linear problem.

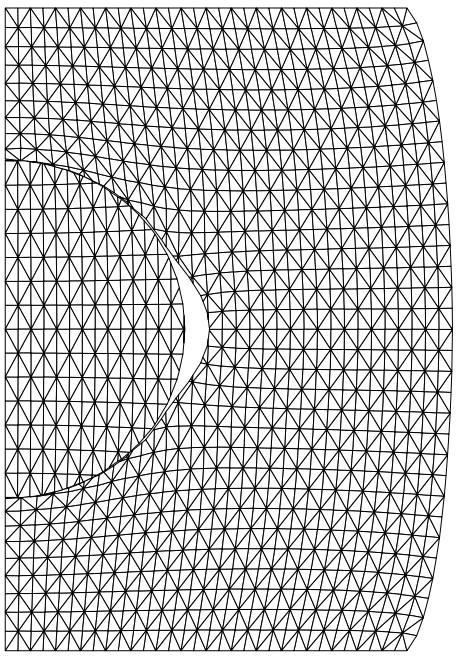

Fig. 4. Displacements for the contact problem.

As regards the implementation, we let the crack entering an element cause a discontinuity in the whole of the element. The crack is assumed to follow a straight line through each element until it hits the boundary to the next element. The situation is illustrated in Fig. 5, where the line C–D is the crack, obeying the constitutive relation $[\boldsymbol{u}] = -\boldsymbol{K}\{\boldsymbol{\sigma}(\boldsymbol{u}) \cdot \boldsymbol{n}\}$. The line A–B, along which the solution should be continuous, is handled as an ordinary interface, i.e., with $\boldsymbol{K} = 0$. Note that continuity is enforced at the nodes A and B, which localizes the effect of the discontinuity since then all non-cracked elements can be standard continuous elements. Finally, we remark that a crack ending in the middle of an element can be handled; the terms that weakly enforce continuity would then be integrated only on the uncracked part (varying material data on the interface is handled similarly).

For our numerical example, we choose a domain $(-1,2) \times (-1,2)$, fixed at $y = -1$ and traction free elsewhere. A body force $\boldsymbol{f} = (-10^6, 0)$ is acting on the console, and the data for this problem were chosen as $v = 0.3$, $E = 10^9$ After crack formation, we assumed a residual compliance corresponding to $\alpha = \beta = 5 \times 10^{-9}$. The small compliancy on the crack interface was necessary in order to regularize the problem; the constant strain elements used proved to be very sensitive to the crack tip singularity and we experienced problems in getting any useful information out of the stresses for large values of α and β. This typically results in the crack turning back on itself. We believe that the origin of this behavior lies in the poor approximation supplied by the constant strain element. The stresses could conceivably be post-processed in order to alleviate this problem, but since the stresses are singular (or at least rapidly varying) at the crack tip there is certainly a need for special approximations in the vicinity of this location (cf. [5]). Such approximations can very conveniently be invoked using the discontinuous Galerkin concept already inherent in the method, although this is beyond the scope of this paper. An alternative possibility in the case of brittle cracks could be to use energy methods, such as the J-integral, which do not require a good resolution at the crack tip.

In Fig. 6 we show the successive growth of a crack forcefully initiated at $x = 2$, $y = 0.72$.

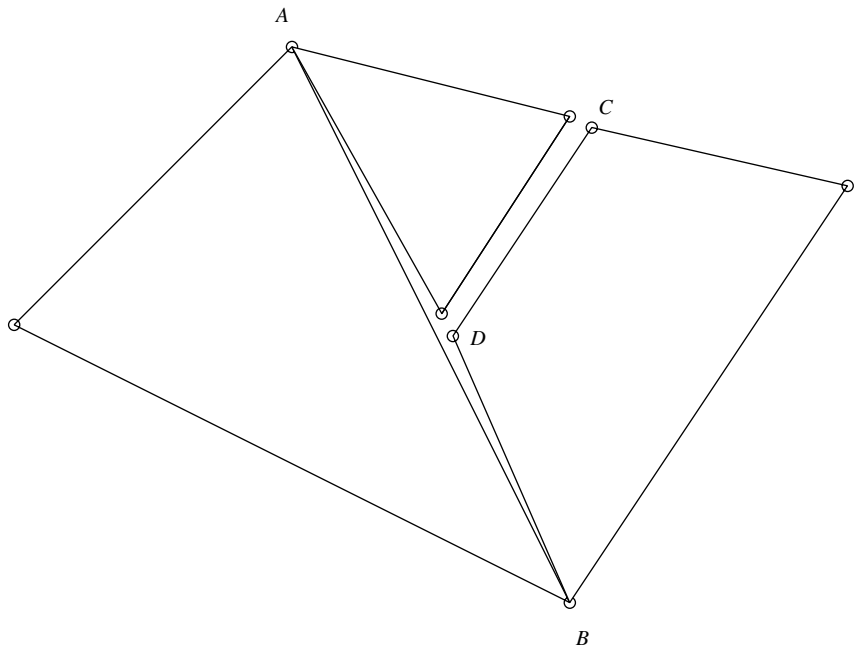

Fig. 5. Illustration of the handling of a cracked element.

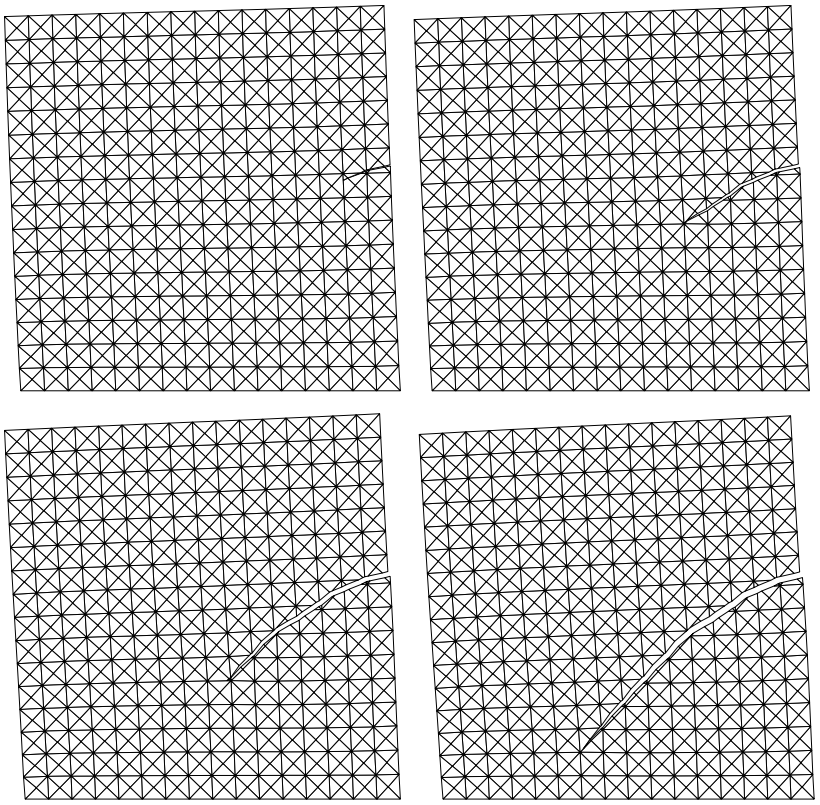

Fig. 6. Crack propagation.

6. Concluding remarks

We have suggested a new discontinuous finite element approach for the simulation of weak and strong discontinuities in linear and non-linear elasticity. The method has been shown to have optimal convergence in the linear case, under the usual regularity requirements. Unlike the current mainstream approaches, our method requires only piecewise polynomial *ansatz* functions, though special purpose approximations can easily be incorporated.

For non-linear problems, such as contact and crack propagation, we have given formulations and examples in model situations. These serve to show the potential of the methodology; future work will focus on more realistic models.

References

[1] I. Babuška, The finite element method for elliptic equations with discontinuous coefficients, Computing 5 (1970) 207–213.
[2] T. Belytschko, N. Möes, S. Usui, C. Parimi, Arbitrary discontinuities in finite elements, Int. J. Numer. Methods Engrg. 50 (2001) 993–1013.
[3] J.H. Bramble, T. Dupont, V. Thomée, Projection methods for Dirichlet's problem in approximating polygonal domains with boundary-value corrections, Math. Comput. 26 (1972) 869–879.
[4] A. Hansbo, P. Hansbo, An unfitted finite element method, based on Nitsche's method, for elliptic interface problems, Comput. Methods Appl. Mech. Engrg. 191 (2002) 5537–5552.

[5] B.L. Karihaloo, Q.Z. Xiao, Modelling of stationary and growing cracks in FE framework without remeshing: a state-of-the-art review, Comput. Struct. 81 (2003) 119–129.
[6] D. Leguillon, E. Sanchez-Palencia, Computation of Singular Solutions in Elliptic Problems and Elasticity, Wiley, 1987.
[7] J. Nitsche, Über ein Variationsprinzip zur Lösung von Dirichlet-Problemen bei Verwendung von Teilräumen, die keinen Randbedingungen unterworfen sind, Abh. Math. Sem. Univ. Hamburg 36 (1971) 9–15.
[8] N. Sukumar, D.L. Chopp, N. Möes, T. Belytschko, Modeling holes and inclusions by level sets in the extended finite-element method, Comput. Methods Appl. Mech. Engrg. 190 (2001) 6183–6200.
[9] G.N. Wells, L.J. Sluys, A new method for modelling cohesive cracks using finite elements, Int. J. Numer. Methods Engrg. 50 (2001) 2667–2682.
[10] Z. Zhong, S.A. Meguid, On the imperfectly bonded spherical inclusion problem, J. Appl. Mech. 66 (1999) 839–846.